Supplemental material for **Nitrogen p-type doping in polycrystalline zinc selenide telluride films**

Christopher P. Muzzillo,[1*] Craig L. Perkins,[1] Sachit Grover,[2] and Andriy Zakutayev[1]

[1]National Laboratory of the Rockies, Golden, CO 80401

[2]California Technology Center, First Solar Inc., Santa Clara, CA 95050

*Corresponding author email: christopher.muzzillo@nrel.gov

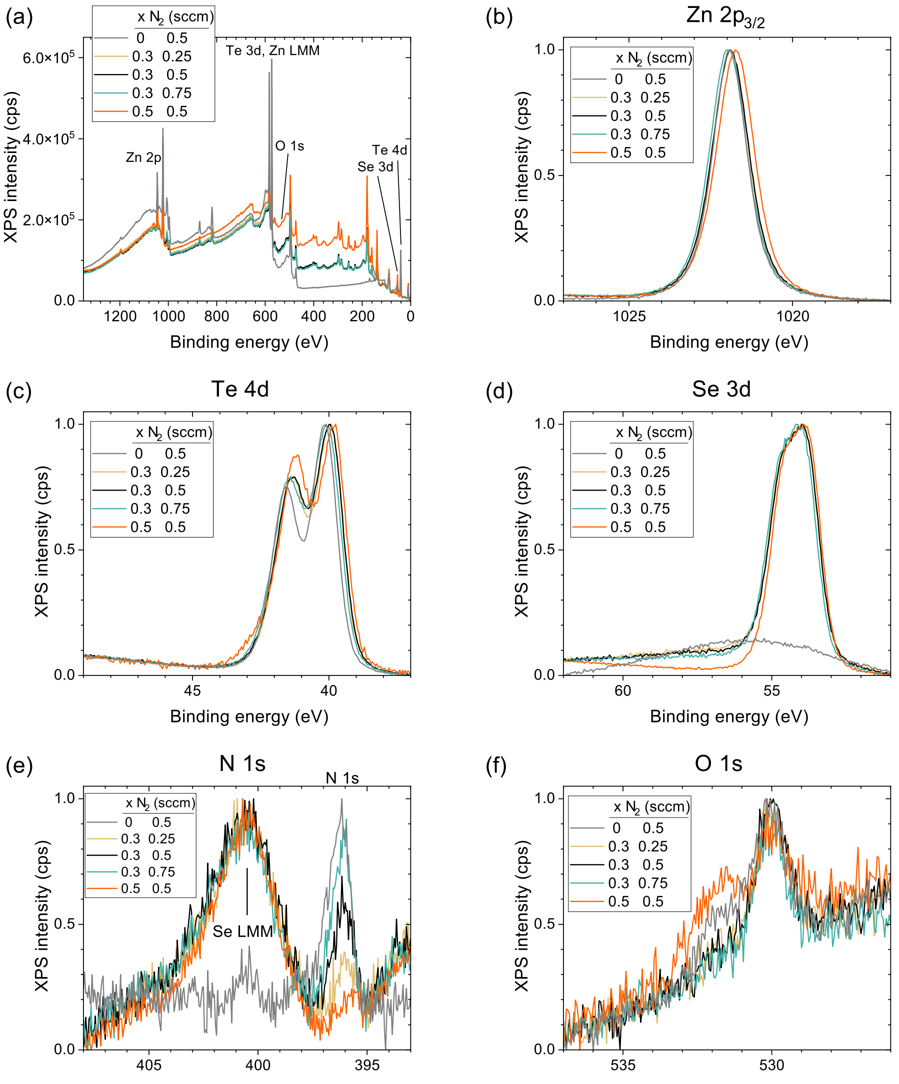

Fig. S1. (a) XPS survey scans, (b) Zn 2p$_{3/2}$, (c) Te 4d, (d) Se 3d, (e) N 1s, and (f) O 1s high resolution core levels of the sputter-cleaned surfaces of ZnSe$_x$Te$_{1-x}$ grown at 370 °C with x of 0, 0.3, and 0.5, and N$_2$ flow rates of 0.25, 0.5, and 0.75 for x of 0.3.

Table S1. XPS compositions for a growth temperature of 370 °C.

XRF x or Se/(Se+Te)	0	0.35	0.36	0.38	0.51
N_2 (sccm)	0.5	0.25	0.5	0.75	0.5
XPS N (%)	2.5	0.63	1.3	2.5	0.43
XPS x or Se/(Se+Te)	0	0.47	0.49	0.53	0.85

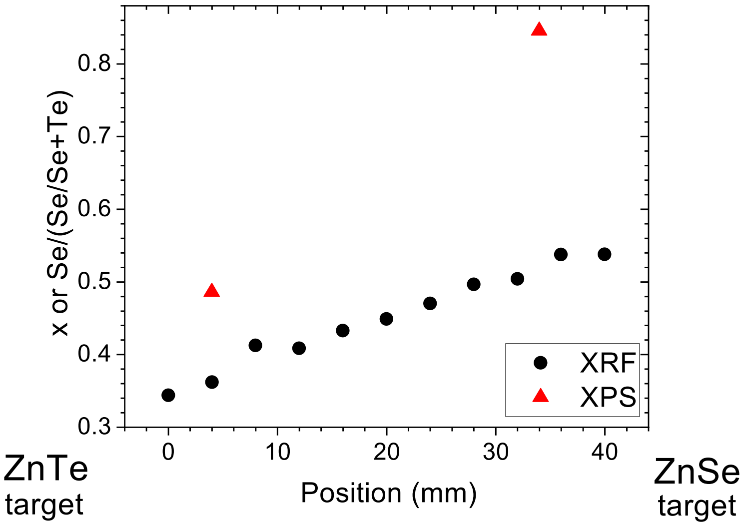

Fig. S2. XRF (black circles) and XPS (red triangles) x or Se/(Se+Te) composition as a function of position on a substrate for a growth temperature of 370 °C and N_2 flow of 0.5 sccm, where the ZnTe target and ZnSe target labels show target locations.

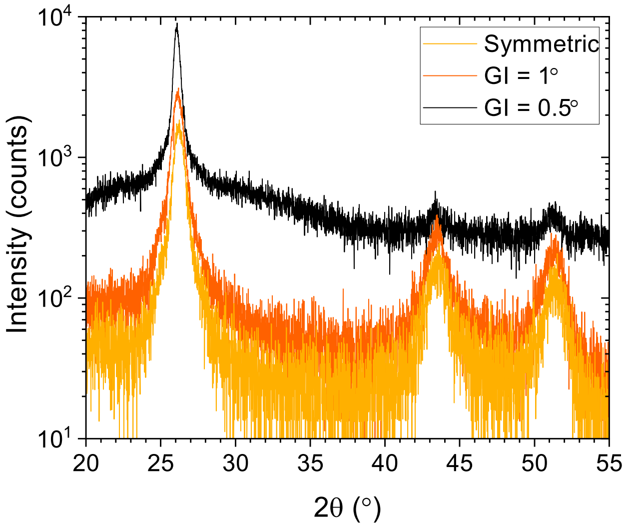

Fig. S3. Symmetric (black) XRD and GIXRD with an incidence angle of 1° (orange) and 0.5° (yellow) for a sample with x of 0.36, N_2 flow of 0.25 sccm, and growth temperature of 370 °C, showing no peak shift or apparent composition change from the bulk of the film to the surface.

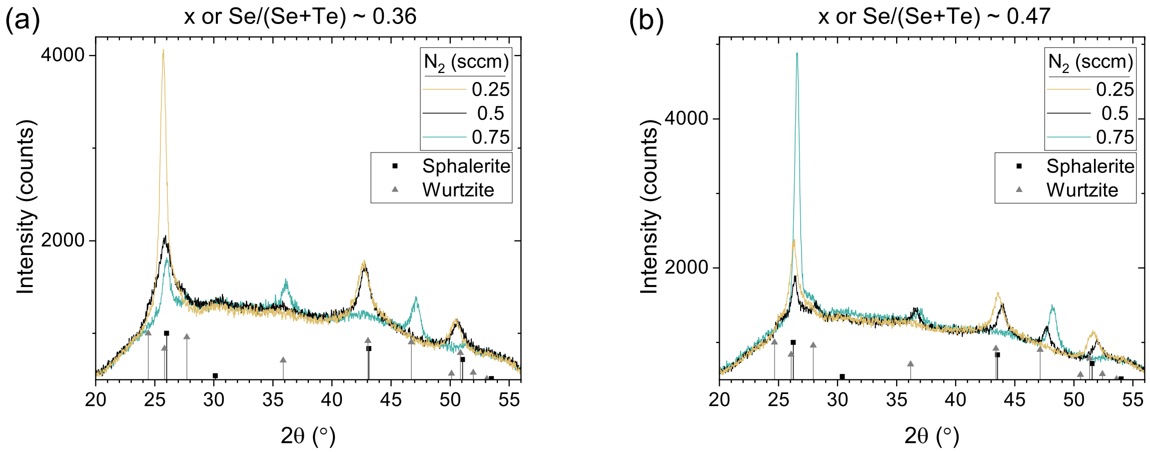

Fig. S4. XRD of films with x of 0.36 (a) and 0.47 (b) and N_2 of 0.25 (yellow), 0.5 (black), and 0.75 (green) sccm for a growth temperature of 370 °C, along with calculated sphalerite (black squares) and wurtzite (gray triangles) peaks, showing that the N_2 stabilizes wurtzite relative to sphalerite at moderate x.

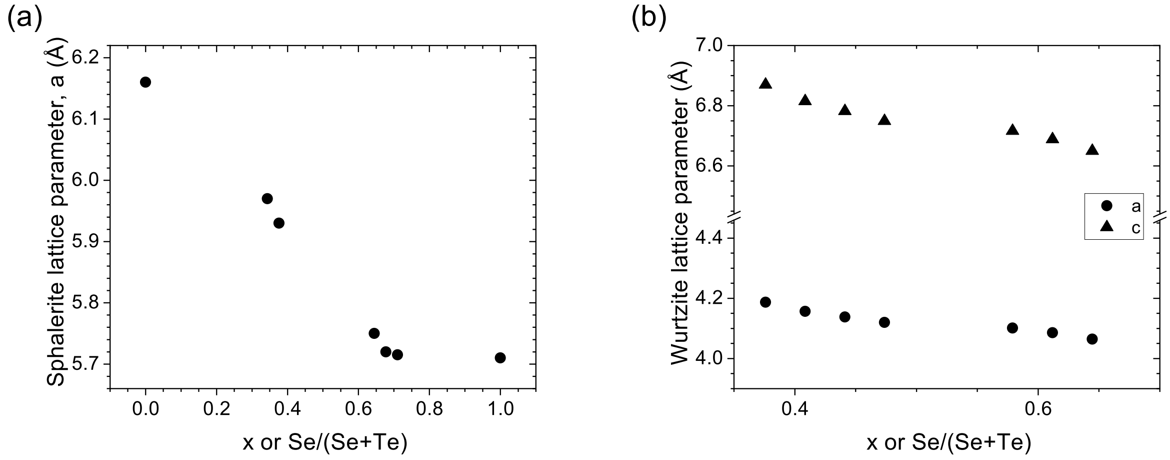

Fig. S5. (a) Sphalerite lattice parameters fit to samples with N_2 flow of 0.5 sccm grown at 370 °C without significant wurtzite, showing sphalerite is stable at low and high x, and the lattice parameter stops shifting around x of 0.67. (b) Wurtzite a (circles) and c (triangles) lattice parameters for samples with N_2 flow of 0.5 sccm grown at 370 °C.

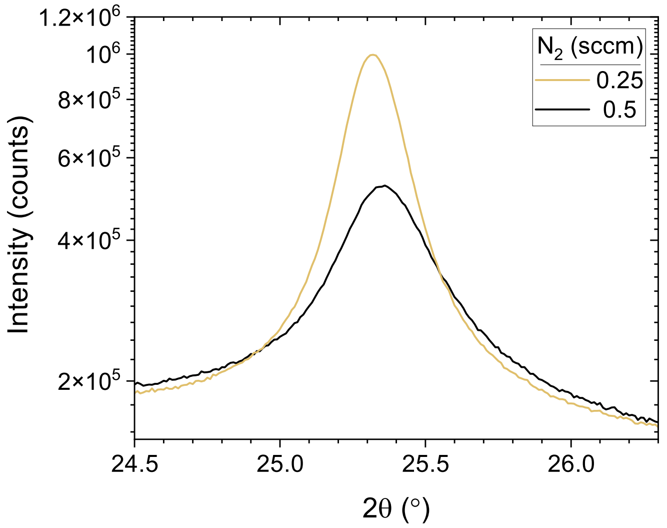

Fig. S6. Magnified (111) XRD peak for x of 0 and N_2 flow of 0.25 (yellow) and 0.5 (black) at a growth temperature of 370 °C, showing a shift to larger full width at half maximum and smaller lattice spacing with N_2 flow.

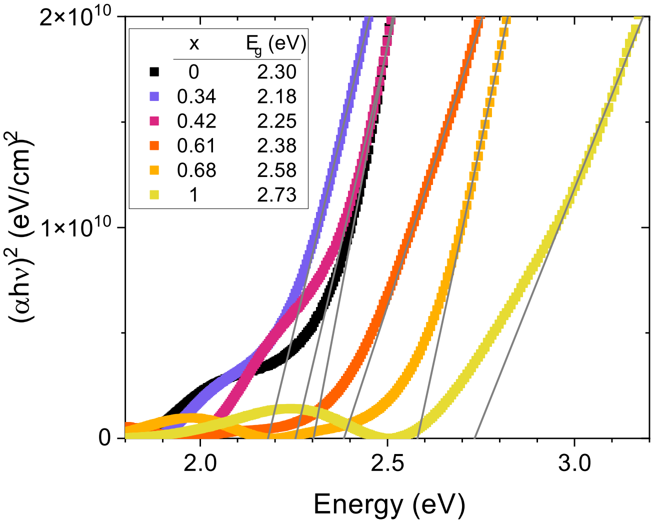

Fig. S7. UV-visible spectroscopy Tauc plot for films with x of 0 (black; 2.30 eV), 0.34 (purple; 2.18 eV), 0.42 (magenta; 2.25 eV), 0.61 (red orange; 2.38 eV), 0.68 (orange; 2.58 eV), and 1 (yellow; 2.73 eV) and N_2 of 0.5 sccm grown at 370 °C, with linear fits extrapolated to band gaps (E_g), showing more band gap bowing than the log10 absorption coefficient plot. Once the y-data reach 0, they increase again at lower energy (depending on film thickness), which is an artefact from film smoothness-caused interference fringes.

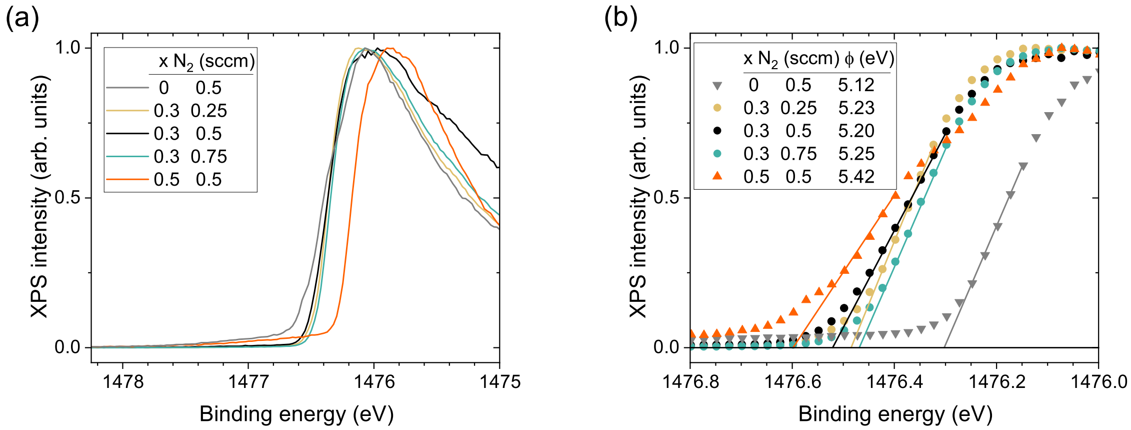

Fig. S8. Low power x-ray excited secondary electron cut-off spectra for x and N_2 flow of 0 and 0.5 (gray triangles), 0.3 and 0.25 (yellow circles), 0.3 and 0.5 (black circles), 0.3 and 0.75 (green circles), and 0.5 and 0.5 (orange triangles) grown at 370 °C, respectively, where the fit x = 0 intercepts are ϕ after calibrating to clean Au foil.

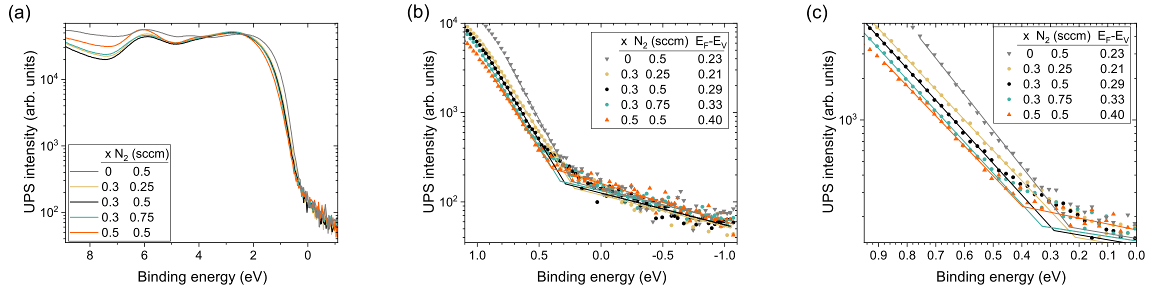

Fig. S9. Log UPS data for x and N_2 flow of 0 and 0.5 (gray triangles), 0.3 and 0.25 (yellow circles), 0.3 and 0.5 (black circles), 0.3 and 0.75 (green circles), and 0.5 and 0.5 (orange triangles) grown at 370 °C, respectively, where the fit intercepts are E_F-E_V.